Journal of Applied Electrochemistry **32**: 1193–1200, 2002.

Influence of different anions on the behaviour of aluminium in aqueous solutions

E. VAN GHEEM*, J. VEREECKEN and C. LE PEN
Department of Metallurgy, Electrochemistry and Materials Science, Vrije Universiteit Brussel, Pleinlaan 2, B-1050 Brussels, Belgium
*(*author for correspondence, fax: +32 2 629 32 00, e-mail: evgheem@vub.ac.be)*

Received 18 December 2001; accepted in revised form 18 June 2002

Key words: aluminium, open circuit potential, pitting corrosion, pitting potential, precipitates

Abstract

The influence of chloride, sulfate and perchlorate anions on the behaviour of native oxide layers on aluminium is investigated using electrochemical techniques. Due to its influence on the open circuit potential and the cathodic side of the polarization curve the oxygen concentration has been carefully controlled. Two kinds of attack on a commercially pure aluminium (99.5 wt %) have been observed. In all the investigated 0.5 M Cl^-, 0.5 M ClO_4^- and 0.5 M SO_4^{2-} aqueous solutions the metal is corroded around the iron and silicon containing precipitates, but only in Cl^- and ClO_4^- solutions is crystallographic pitting observed. Comparison with high purity aluminium (99.99 wt %) shows that pitting corrosion is not influenced by the presence of impurities in the aluminium alloys, but by the presence of anions in solution. The pH and/or oxygen concentration determine whether or not the pitting potential coincides with the corrosion potential.

1. Introduction

The behaviour of aluminium and aluminium alloys in aqueous environments depends on several parameters, such as the solution composition (pH, nature and concentration of anions, oxygen concentration etc.) [1]. Even crystal orientation [2], as well as the structure and composition of the oxide layer which, in their turn are influenced by mechanical and heat treatments, have an influence on the corrosion behaviour of aluminium alloys. Therefore it is sometimes difficult to evaluate published results since the experimental conditions are not always clearly defined.

Many studies have been devoted to the electrochemical behaviour of aluminium alloys in NaCl solutions [1–18]. All these studies reveal that the exposure of aluminium alloys to chloride ions results in localized corrosion (crystallographic pitting corrosion). From some of these investigations [3–6] it can be concluded that in an aerated solution the pitting potential (E_{pit}) is equal to the corrosion potential (Table 1). This is not the case in deaerated chloride solutions. In deaerated conditions most of the measurements show values around −1.2 V vs SCE for the corrosion potential [3, 7, 9–11], whereas the reported pitting potentials do not differ greatly from those for the aerated chloride solutions [3, 8–11]. Despite the importance of the oxygen concentration it has not always been mentioned whether the measurement is carried out in a deaerated or aerated solution [12–14]. Different mechanisms for pitting corrosion in a chloride solution can be found in the literature. A possible mechanism is aluminium dissolution [1, 11, 14, 19, 20] followed by reaction with chloride ions [1, 14, 19, 20]. Some authors [14, 20] observe that the oxide layer contains microfissures and defects, allowing chloride ions to enter and access the bare metal. Bockris et al. [21] provide strong indications that the oxide layer contains AlOOH fibrils. They suggest that these fibrils can be considered as crystal imperfections in the passive film where chlorides can easily enter. Both mechanisms are tenable since XPS analysis and radiotracer techniques reveal the incorporation of Cl^- ions into the oxide film [4, 15].

The Cl^- solution pH is another important parameter. To what extend the solution pH acts upon the open circuit potential and/or corrosion potential is not clear, since reported values are not consistent (Table 1) [7, 16, 25]. Liao et al. [16] report that the open circuit potential of aerated Cl^- solution changes dramatically when its pH is reduced from 6.5 to 3.5. Dražić et al. [9] conclude that a decrease in pH increases the corrosion rate.

The influence of SO_4^{2-} ions on aluminium alloys has been a subject of many studies [3, 5, 7, 12, 13, 15, 18, 19, 22–24]. Some of these indicate values for the corrosion potential (Table 1) [3, 7, 12, 22, 24]. From the few available data it can be concluded that the corrosion potential depends on whether the solution is aerated or deaerated. It is observed (Table 1) [3] that the corrosion

Table 1. Summary of the literature results

Metal	Solution	pH	E_{cor} or **OCP** vs SCE /V	E_{pit} vs SCE /V	Aerated	Deaerated	Reference
Al 99.999%	0.6 M NaCl	?	?	(110) −0.708 (100) −0.729 (111) −0.735		*	[2]
Pure Al	0.3 M Na_2SO_4	?	−1.05	–		*	[3]
			−0.60	–	*		
	0.6 M NaCl (NaOH add.)	7	−1.20	−0.75		*	
			−0.75	−0.75	*		
Pure Al	0.5 M NaCl	?	−0.72	−0.72	*		[4]
Al 99.999%	0.1 M NaCl	?	−0.75	−0.70	*		[5]
Al 99.99%	3% NaCl	?	−0.72	−0.72	*		[6]
Al 99.999%	1 M NaCl	?	−1.020	?		*	[7]
	1 M HCl	?	−0.825	?		*	
	0.5 M H_2SO_4	?	−0.868	?		*	
Al 99.99%	0.1 M NaCl	?	?	−0.64		*	[8]
	0.1 M $NaClO_4$	?	?	−0.24		*	
	0.5 M NaCl	?	?	−0.74		*	
Al 99.999%	0.5 M NaCl	6.5	−1.15	−0.75		*	[9]
Al 99.7 min	0.085 M NaCl	?	?	−0.67		*	[10]
	0.6 M NaCl	6.4	−1.25	?		*	
Al-Fe alloy (1.4%Fe)	0.5 M NaCl	?	−0.75	−0.73		*	[11]
Al 99.999%	3% NaCl	?	−1.041	?	?	?	[12]
	0.3% Na_2SO_4	?	−0.890	–	?	?	
Al 99.999%	0.01 M NaCl	?	−0.76	−0.49	?	?	[13]
Al	0.1 M $KClO_4$	?	?	−0.40	?	?	[14]
	1 M NaCl	?	?	−0.74	?	?	
Al 99.999%	0.1 M $NaClO_4$	?	?	−0.66	?	?	[15]
Pure Al	0.5 M NaCl	6.5	**−0.73**	?	*		[16]
		3.5	**−1.15**	?	*		
	0.7 M NaCl	3.5	**−1.15**	?	*		
Al(CP)	1 M NaCl	?	?	−0.71	*		[17]
Al 99.99%	0.01 M Na_2SO_4	7	−1.49	–		*	[22]
Al 99.99%	0.5 M Na_2SO_4	?	−0.65	–	?	?	[24]
Pure Al	0.1 M HCl	?	−0.94	−0.73	*	*	[25]

potential of neutral SO_4^{2-} solutions is −1.05 V vs SCE under aerated conditions and −0.60 V vs SCE under deaerated conditions. In deaerated 0.5 M H_2SO_4 solution the corrosion potential (based on only one reference) is −0.87 V vs SCE (Table 1) [7]. Sulfate, added to Cl^- solutions, seems to inhibit corrosion [5, 13]; this can be explained by preferential adsorption of the SO_4^{2-} ions at the oxide film [15, 23]. This hypothesis is confirmed by Kolics et al. using radiotracer techniques [15] and by Isaacs et al. who applied cyclic voltammetry [23].

Fewer studies have been published on the influence of perchlorate ions on aluminium. These ions are often used as a supporting electrolyte [15], although aluminium is attacked in these solutions [8, 14, 15]. The pitting tendency is less pronounced than in chloride solutions [8]. XPS analysis shows the presence of chloride in the oxide film. This indicates that there may be a small extent of transformation of perchlorate to chloride in the oxide film [15]. Szklarska–Smialowska reports that the pitting potentials of aluminium in neutral and acid perchlorate solution differ very little, being more negative in acid than in alkaline solution [14].

The objective of this work is to obtain further information on the behaviour of aluminium in chloride, sulfate and perchlorate solutions in relation to oxygen concentration and pH. For this purpose the open circuit potential of aluminium is measured in these solutions as a function of time, polarization curves are recorded and SEM observation is carried out. The influence of impurities (e.g., Fe and Si) in the metal is also investigated by comparing the behaviour of commercially pure aluminium (AA1050; 99.5 wt %) with the pure metal (99.99 wt %).

2. Experimental details

Two grades of aluminium sheets were used: aluminium alloy AA1050 (composition: Table 2) and pure aluminium (composition: Table 2). Both grades are produced by Vereinigde Aluminium-Werke, Germany. Prior to each experiment, the surface of the samples was etched in 10 wt % NaOH solution for 20 s at 60 °C. Then the specimens were rinsed with deionized water, immersed in 10 wt % HNO_3 solution for 60 s at 60 °C, rinsed again with deionized water and dried in cold air. This pretreatment was to obtain a reproducible surface composition. The exposed area of the working electrode

Table 2. Composition of the investigated aluminium alloy and the high purity aluminium

Metal	Alloy composition/wt %										
	Al	Si	Fe	Cu	Mn	Mg	Zn	V	Ti	B	Others
AA1050	99.5	0.25	0.4	0.05	0.05	0.05	–	0.05	–	–	0.03 (each)
High purity	99.99	0.003	0.0042	0.0021	0.0004	–	0.0009	–	0.0018	0.0004	–

was 1.13 cm^2. A platinum wire and a saturated calomel electrode (SCE) were used, respectively, as counter and reference electrode.

The electrolytes were prepared from proanalysis chemicals and deionized water. The concentration of the solutions was always 0.5 M, since experiments using this concentration are the most described in the literature and are therefore useful as references. The solutions were bubbled with oxygen gas or nitrogen gas (purities: Table 3) for 30 min to increase or reduce the oxygen concentration. During the measurement the solution was continuously bubbled with a gas flow of 60 l h^{-1}. This gas flow was chosen to meet two objectives: a constant oxygen concentration of either 40 ppm or <0.1 ppm and a good stirring of the solution. Then the open circuit potential was recorded as a function of time for 8000 s with an Autolab Instruments of Ecochemie PGSTAT10 potentiostat. These 8000 s were necessary to reach a constant open circuit potential. Subsequently a potentiodynamic polarization curve was recorded at a scan rate of 0.5 mV s^{-1}, from −1.4 V vs SCE to maximum +1.4 V vs SCE. The data were acquired by a Compaq Prolinea 4/66 computer, using the software program GPES developed by Ecochemie.

To observe the morphology of the tested specimens use was made of a Jeol scanning electron microscope (SEM) type JSM6400 in combination with the software program Adobe premiere 5.1.

3. Results

3.1. *Open circuit potential as a function of time*

Table 4 shows the open circuit potentials of AA1050 and high purity aluminium after 8000 s immersion under different conditions. In the aerated neutral solutions the following values for the open circuit potential of AA1050 were measured: −0.75 V vs SCE in 0.5 M NaCl, −0.51 V vs SCE in 0.5 M K_2SO_4 and −0.48 V vs SCE in 0.5 M $NaClO_4$. Deaeration of the neutral solutions shifts the open circuit potential of AA1050 towards less positive values (−0.95 V vs SCE in 0.5 M NaCl, −1.02 V vs SCE in 0.5 M K_2SO_4 and −1.17 V vs SCE in 0.5 M $NaClO_4$).

Under aerated conditions, the open circuit potential of AA1050 hardly changes with pH, for all tested anions. This is not the case for the deaerated solutions. The behaviour of high purity aluminium has been

Table 3. Purity of used gases

Gas	Purity/%	Impurity				
		CH_4/ppm	Ar/%	H_2O/ppm	O_2/ppm	H_2/ppm
O_2	99	40	1	–	–	–
N_2	99.999	–	–	5	3	1

Table 4. The open circuit potential after 8000 s of immersion in the solution

Metal	Solution	Gas	pH before the electrochemical experiment	OCP vs SCE /V after 8000 s
AA1050	0.5 M NaCl	O_2	5.6	−0.75
		N_2	5.6	−0.95
	0.5 M K_2SO_4	O_2	6.0	−0.51
		N_2	6.0	−1.02
	0.5 M $NaClO_4$	O_2	6.9	−0.48
		N_2	6.8	−1.17
	0.5 M HCl	O_2	0.5	−0.77
		N_2	0.4	−0.88
	0.5 M H_2SO_4	O_2	0.4	−0.55
		N_2	0.4	−0.80
	0.5 M $HClO_4$	O_2	0.3	−0.45
		N_2	0.3	−0.84
High purity Al	0.5 M NaCl	O_2	5.7	−1.12
		N_2	5.7	−1.41

investigated only in neutral chloride solutions. Measurements showed an open circuit potential of −1.12 V vs SCE in the aerated solution and of −1.41 V vs SCE in the deaerated one.

3.2. *Potentiodynamic polarization curves*

The most important characteristic values derived from the potentiodynamic polarization curves are given in Table 5.

3.2.1. *Potentiodynamic polarization curves in neutral solutions*

Figure 1 shows the polarization curves of AA1050 in aerated neutral solutions. The values of the corrosion potential in 0.5 M NaCl and in 0.5 M $NaClO_4$ solution coincide with their open circuit potential (Table 4).

The shape of the cathodic branches is nearly the same in the three solutions. The point of intersection of the tangent lines to the cathodic and anodic branches at the corrosion potential yields i_{corr}. This current density is much higher in the NaCl solution ($\sim 10^{-5}$ A cm^{-2}) than in the two others ($\sim 10^{-7}$ A cm^{-2}). Above the corrosion potential the current density increases sharply in the NaCl solution, reaching about 0.1 A cm^{-2} at 0 V vs SCE. During recording of the anodic side of the polarization curve, small gas bubbles were formed at the electrode surface. In the two other solutions the current density reaches a plateau above the corrosion potential, at nearly the same value ($\sim 3 \times 10^{-6}$ A cm^{-2}). At −0.12 V vs SCE in ClO_4^- solution and at 0.4 V vs SCE in SO_4^{2-} solution the plateau ends and from there on the current density increases.

The corrosion potentials obtained from the potentiodynamic polarization curves of AA1050 in deaerated neutral solutions (Figure 2) coincide with the open circuit potential measured after immersing for 8000 s (Table 4). The cathodic branches of the polarization curve of AA 1050 in the SO_4^{2-} and ClO_4^- solutions fall together, but in the Cl^- solution higher current densities are measured in the potential range from −1.06 to −1.32 V vs SCE.

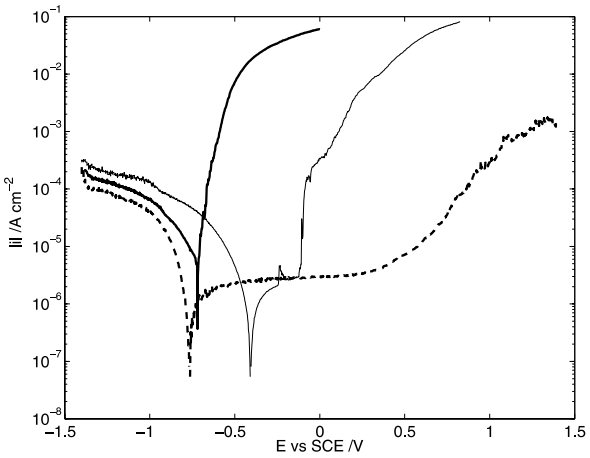

Fig. 1. Potentiodynamic polarization curves of AA1050 with oxygen bubbling in 0.5 M NaCl(—), 0.5 M K_2SO_4(– – –) and 0.5 M $NaClO_4$(—).

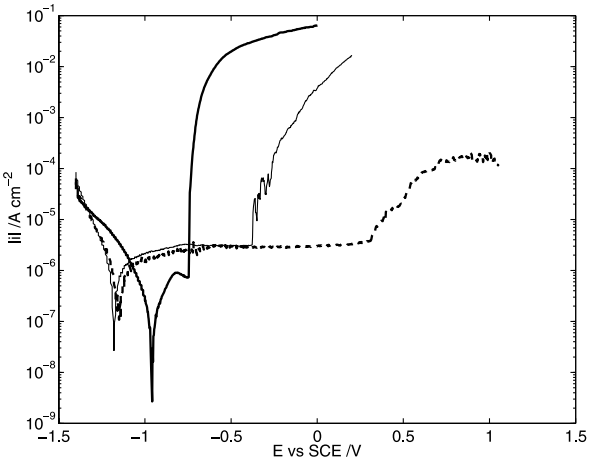

Fig. 2. Potentiodynamic polarization curves of AA1050 with nitrogen bubbling in 0.5 M NaCl(—), 0.5 M K_2SO_4(– – –) and 0.5 M $NaClO_4$(—).

In the deaerated neutral solutions i_{corr} in the SO_4^{2-} and ClO_4^- solution is identical (2×10^{-7} A cm^{-2}). In the

Table 5. Summary of results conducted from the polarization curves

Metal	Solution	pH after the polarization curve	E_{cor} vs SCE/V	E_{pit} vs SCE/V	Aerated	Deaerated
AA1050	0.5 M NaCl	8.2	−0.72	−0.72	*	
		8.2	−0.96	−0.75		*
	0.5 M K_2SO_4	9.0	−0.76	–	*	
		8.2	−1.15	–		*
	0.5 M $NaClO_4$	7.9	−0.41	−0.12	*	
		7.0	−1.18	−0.38		*
	0.5 M HCl	0.5	−0.77	−0.77	*	
		0.4	−0.84	−0.84		*
	0.5 M H_2SO_4	0.4	−0.54	–	*	
		0.4	−0.80	–		*
	0.5 M $HClO_4$	0.4	−0.40	−0.40	*	
		0.3	−0.82	−0.40		*
Al 99.99%	0.5 M NaCl	8.2	−1.14	−0.74	*	
		8.2	−1.43	−0.74		*

deaerated chloride solution a ten times lower value (2×10^{-8} A cm^{-2}) is measured.

In the absence of oxygen the corrosion potential is shifted negatively in all solutions. The passivation current densities in deaerated perchlorate and sulfate solution are not influenced by oxygen concentration. At -0.4 V vs SCE in the ClO_4^- solution and only at 0.3 V vs SCE in the SO_4^{2-} solution the current density increases. In deaerated Cl^- solution the current density shows a kind of plateau in the range from -0.96 to -0.75 V vs SCE. Beyond -0.75 V vs SCE the current density rises sharply.

3.2.2. *Potentiodynamic polarization curves in acid solutions*

Figure 3 shows the polarization curves of AA1050 in the aerated acid solutions. The shape of the cathodic branch is almost the same in the three solutions and they all show a point of inflection. The corrosion potentials are equal to the open circuit potentials mentioned in Table 4.

Acidification of the aerated solutions increases the corrosion current densities of AA1050: $i_{corr\ HCl} \approx 7 \times 10^{-4}$ A cm^{-2}; $i_{corr\ HClO_4} \approx 10^{-4}$ A cm^{-2}; $i_{corr\ H_2SO_4} \approx 3 \times 10^{-5}$ A cm^{-2}. Immediately above the corrosion potential the current density increases sharply in the chloride and perchlorate solution, reaching a maximum of 0.3 A cm^{-2} and 0.18 A cm^{-2} respectively. In the SO_4^{2-} solution the anodic branch exhibits a plateau at about 10^{-3} A cm^{-2} from about -0.4 V vs SCE.

The corrosion potential of AA1050 in deaerated acid solutions (Figure 4) is marginally influenced by the nature of the anions (~ -0.82 V vs SCE). The corrosion current density is nearly the same in the chloride and sulfate solution ($\sim 10^{-5}$A cm^{-2}), but is lower in the perchlorate solution ($\sim 10^{-6}$ A cm^{-2}). In the deaerated $HClO_4$ solution the cathodic branch of AA1050 approaches a straight line. Both cathodic branches in the deaerated HCl and H_2SO_4 solutions coincide but have no point of inflection, as is the case for the aerated solutions. The current density in the chloride solution jumps to very high levels ($\sim 10^{-2}$ A cm^{-2}) at potentials closely above the corrosion potential. In the sulfate solution the current density remains low ($\sim 10^{-4}$ A cm^{-2}). In the perchlorate solution the current density increases sharply at -0.40 V vs SCE and coincides, from there on, with the anodic branch of AA1050 in the chloride solution.

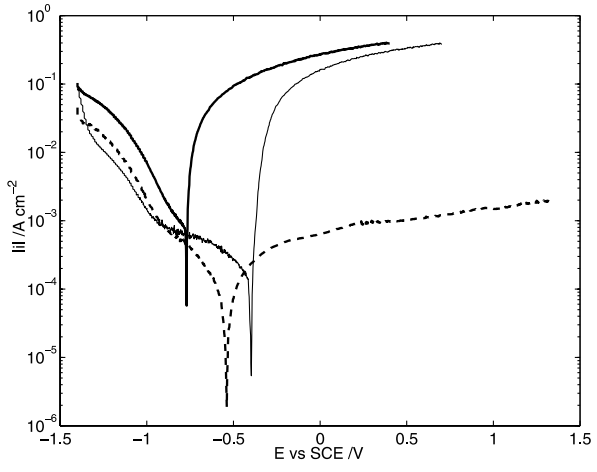

Fig. 3. Potentiodynamic polarization curves of AA1050 with oxygen bubbling in 0.5 M HCl(—), 0.5 M H_2SO_4(– – –) and 0.5 M $HClO_4$(—).

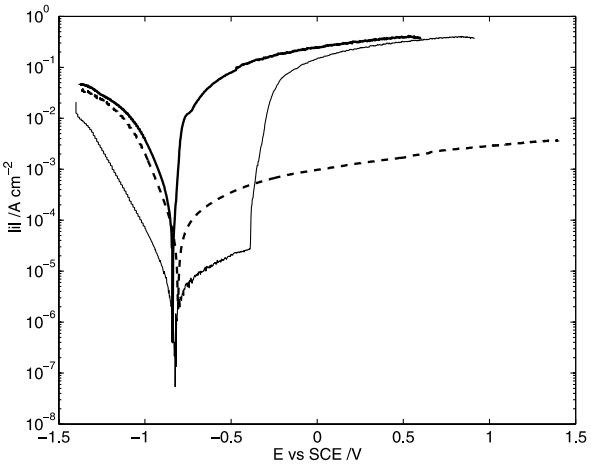

Fig. 4. Potentiodynamic polarization curves of AA1050 with nitrogen bubbling in 0.5 M HCl(—), 0.5 M H_2SO_4(– – –) and 0.5 M $HClO_4$(—).

3.2.3. *Influence of the alloying elements on the potentiodynamic polarization curves in neutral solutions*

Comparing the polarization curves of AA1050 and high purity aluminium in an aerated neutral chloride solution (Figure 5) it is remarkable that although they have different corrosion potentials the current densities rise sharply at the same potential.

3.3. *Morphology of the surface at the open circuit potential*

Figure 6 shows characteristic SEM photographs of samples after the recording of the open circuit potential during 8000 s. Crystallographic corrosion of AA1050

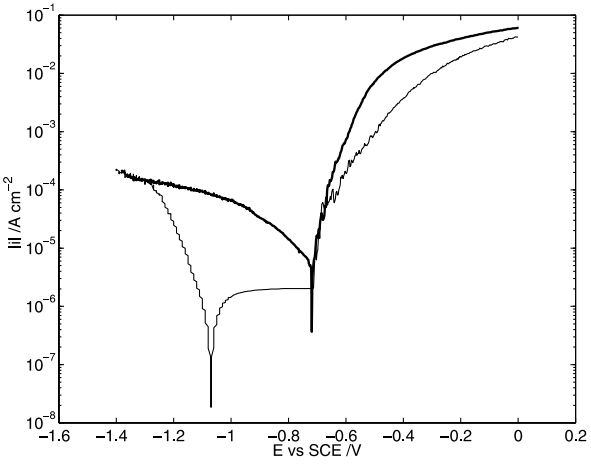

Fig. 5. Potentiodynamic polarization curves of AA1050 (—) and high purity aluminium (—) with oxygen bubbling in 0.5 M NaCl.

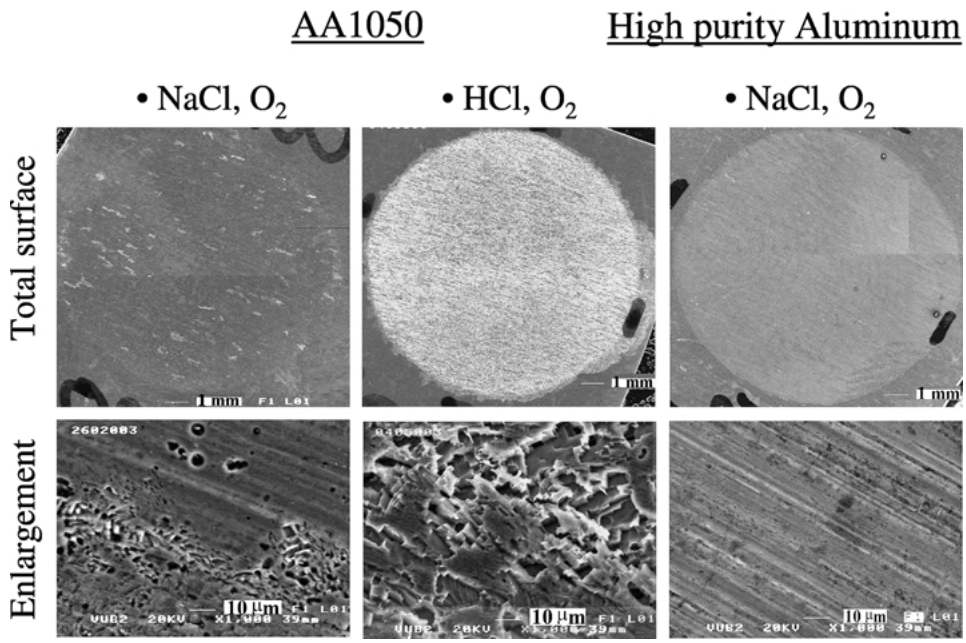

Fig. 6. SEM images of the surface after the recording of the open circuit potential. Left AA1050, right pure aluminium.

was observed after immersion in the following solutions: aerated chloride in neutral as well as acid solutions (Figure 6), deaerated acid chloride solution and aerated acid perchlorate solution. In all other considered solutions crystallographic corrosion was not observed. At a larger magnification the SEM photographs show white spots in black 'holes' at the surface of the AA1050 electrodes after immersion in all the solutions. These white spots in black 'holes' contain iron and silicon (EDX).

When high purity aluminium is immersed in an aerated NaCl solution, no corrosion at all is observed at the open circuit potential (Figure 6).

3.4. *Morphology after the potentiodynamic polarization curves*

AA1050 electrodes exposed to any of the Cl^- and ClO_4^- solutions (neutral (Figure 7), acid, aerated (Figure 7) and deaerated) were completely covered by crystallographic pits, except for neutral ClO_4^- solutions where only partial coverage was noted. No crystallographic corrosion is observed on the AA1050 samples, exposed to any of the SO_4^{2-} solutions (Figure 7).

Pure aluminium exposed to aerated and deaerated neutral Cl^- solutions were in both cases completely covered by crystallographic pits.

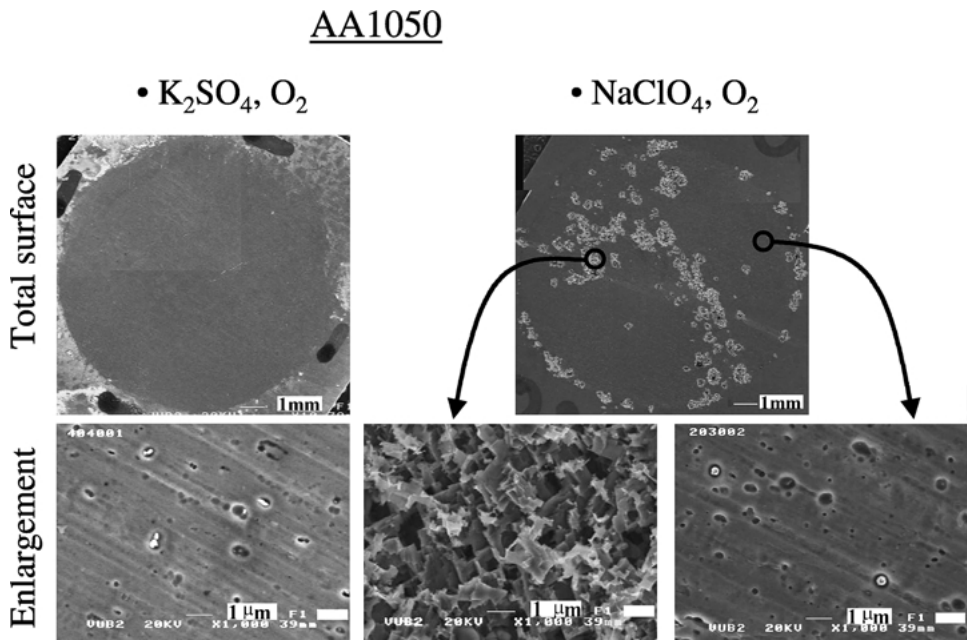

Fig. 7. SEM images of the surface after the recording of the potentiodynamic polarization curve.

All AA1050 samples showed, after exposure to any of the solutions (neutral, acid, aerated and deaerated), the white spots in black 'holes'.

4. Discussion

4.1. *General*

From the experimental data (Table 4) it can be concluded that oxygen bubbling shifts the open circuit potentials towards more positive values, regardless of the type of alloy or solution involved. The magnitude of the shift depends highly on the type of dissolved anion and the pH. This is in line with the findings of Carbonini et al., who did the same kind of investigation but only in neutral solutions (Table 1) [3]. The explanation for the shift has to be found in the nature of reduction reactions that occur at the open circuit potential. In the aerated condition oxygen as well as protons are reduced [9, 11, 14, 20], whereas in the deaerated situation only protons are reduced [1, 3, 9, 15, 22].

SEM photographs, taken of AA1050 samples immersed in aerated and deaerated neutral as well as in acid solutions, at the open circuit potential , show black holes with iron and/or silicon containing precipitates in it. From the literature it is known that the precipitates in AA1050 (predominantly Al_3Fe and α–AlFeSi [18]) are cathodic [16] in comparison to the matrix. Due to this microgalvanic corrosion, the matrix will dissolve at the boundaries of the precipitates.

4.2. *Chloride anions*

SEM photographs were taken of AA1050 samples immersed in 0.5 M aerated and deaerated, neutral as well as acid, chloride solutions, after recording of their open circuit potential. They all show crystallographic pitting corrosion, except for the deaerated neutral solution which shows only microgalvanic corrosion. This observation is in agreement with Uruchurtu's conclusions [6]. Crystallographic pitting of AA1050 in this deaerated neutral chloride solution occurs at a higher potential than the corrosion potential as observed from the recording of the polarization curve (Figure 2).

For high purity aluminium the same tests were carried out in aerated and deaerated neutral chloride solutions. At the open circuit potential no corrosion is observed. Crystallographic corrosion of pure aluminium occurs at the same potential as the open circuit potential of AA1050.

It is important to note that the two grades of aluminium exposed to aerated and deaerated neutral chloride solutions have a different corrosion potential but do exhibit an identical (crystallographic) pitting potential. This indicates that neither the composition of the aluminium alloy (e.g., iron and silicon impurities) nor the presence or absence of oxygen have an influence on the crystallographic corrosion, and that this kind of corrosion is caused by interaction between the anions and the oxide layer.

High purity aluminium exhibits, compared to the AA1050 alloy, a more negative open circuit potential in both aerated and deaerated neutral chloride solutions due to the absence of precipitates.

The open circuit potential of AA1050 in acid solutions is affected by oxygen but much less than in neutral solutions. This observation is not supported by Brett [25], who reports no effect at all. This could be due to the aerated condition.

4.3. *Sulfate anions*

SEM photographs of AA1050 immersed in aerated and deaerated, neutral and acid SO_4^{2-} solutions show microgalvanic corrosion but no crystallographic pitting at whatever potential.

In the neutral and acid sulfate solutions AA1050 shows a passive behaviour. In the neutral solutions the current density starts to rise when the potential exceeds ~0.4 V vs SCE. This can be explained by the evolution of oxygen in aerated as well as deaerated solutions [27]. The open circuit potential of AA1050 in 0.5 M SO_4^{2-} deaerated acid solution is clearly higher than in the neutral solution (Table 4). In the aerated condition the acidification has practically no influence on the open circuit potential (Table 4).

4.4. *Perchlorate anions*

AA1050 dipped for 8000 s in aerated and deaerated 0.5 M $NaClO_4$ and in deaerated $HClO_4$ solutions is not affected by crystallographic pits, but the surface is attacked by microgalvanic corrosion. In aerated $HClO_4$ crystallographic attack as well as galvanic corrosion is noted. However, after recording the potentiodynamic polarization curves in all types of ClO_4^- solutions (aerated deaerated, acid, neutral), AA1050 is crystallographically pitted. It can be concluded that only in the aerated acid ClO_4^- condition does the pitting potential coincide with the corrosion potential. For all other conditions the corrosion potential is less positive than the pitting potential. Acidification only shifts the AA1050 corrosion potential in the deaerated solution to a more positive value.

5. Conclusions

AA1050 alloy, when exposed to all types of Cl^-, ClO_4^- and SO_4^{2-} solutions, is affected by microgalvanic corrosion. This corrosion can be explained by the cathodic character of the precipitates. The AA1050 alloy, when immersed in all types of Cl^- and ClO_4^- solutions, also shows crystallographic corrosion, above a certain potential (E_{pit}). This pitting potential coincides with the corrosion potential in the following cases: aerated

neutral and acid Cl^- solution, aerated acid ClO_4^- solution and deaerated acid chloride solution. In all other cases a passive region is observed. The AA1050 specimens are not crystallographic pitted, when exposed to whatever type of SO_4^{2-} solution.

The corrosion potential of AA1050 in deaerated acid solutions of all considered anions is more positive than in the neutral homologues. Although high purity aluminium does not corrode during immersion in aerated and deaerated neutral chloride solution, it exhibits the same pitting potential as AA1050 when exposed to these solutions. It has also been confirmed that the corrosion potential of aluminium is influenced by the presence of precipitates and/or oxygen concentration.

Finally, this study clearly demonstrates that parameters like oxygen concentration, pH and aluminium grade have to be accurately controlled to be able to compare the influence of different anions on the behaviour of aluminium in aqueous solutions.

References

1. N. Lampeas and P.G. Koutsoukos, *Corros. Sci.* **36** (1994) 1011.
2. B.W. Davis, P.J. Moran and P.M. Nathishan, *Proc. Electrochem. Soc.* **98-17** (1998) 215.
3. P. Carbonini, T. Monetta, D.B. Mitton, F. Bellucci, P. Mastronardi and B. Scatteia, *J. Appl. Electrochem.* **27** (1997) 1135.
4. L. Garrigues, N. Pebere and F. Dabosi, *Electrochim. Acta* **41** (1996) 1209.
5. S-I. Pyun, K-H. Na, W-J. Lee and J.-J. Park, *Corrosion* **56** (2000) 1015.
6. J. Uruchurtu Chavarin, *Corrosion* **47** (1991) 472.
7. A.A. Aksüt and G. Bayramoğlu, *Corros. Sci.* **36** (1994) 415.
8. H. Böhni and H.H. Uhlig, *J. Electrochem. Soc.: Electrochem. Sci.* **116** (1969) 906.
9. D.M. Dražić and J.P. Popić, *J. Appl. Electrochem.* **29** (1999) 43.
10. W.J. Rudd and J.C. Scully, *Corros. Sci.* **20** (1980) 611.
11. O. Seri, *Corros. Sci.* **36** (1994) 1789.
12. A. Barbucci, G. Bruzzone, M. Delucchi, M. Panizza and G. Cerisola, *Intermetallics* **8** (2000) 305.
13. W-J. Lee and S-I. Pyun, *Electrochim. Acta* **45** (2000) 1901.
14. Z. Szklarska-Smialowska, 'Pitting corrosion of metals', National Association of Corrosion Engineers, Houston, TX (1986).
15. A. Kolics, J.C. Polkinghorne and A. Wieckowski, *Electrochim. Acta* **43** (1998) 2605.
16. C-M. Liao and R.P. Wei, *Electrochim. Acta* **45** (1999) 881.
17. N. Myung, L. Chen, E-H. Chung and K. Nobe *Proc. Electrochem. Soc.* **98-17** (1998) 165.
18. K. Niosancioğlu, K. Yngve Davanger ϕ. Strandmyr, *J. Electrochem. Soc.* **128** (1981) 1523.
19. R.T. Foley and T.H. Nguyen, *J. Electrochem. Soc.* **129** (1982) 464.
20. A.K. Vijh, *Corros. Sci.* **36** (1994) 1615.
21. J.O'M. Bockris and Y. Kang, *J. Solid State Electrochem.* **1** (1997) 17.
22. A.H. Al-Saffar, V. Ashworth, A.K.O. Bairamov, D.J. Chivers, W.A. Grant and R.P.M. Procter, *Corros. Sci.* **20** (1980) 127.
23. H.S. Isaacs, F. Xu and C.S. Jeffcoate, *Proc. Electrochem. Soc.* ('Passivity and Localized Corrosion') **99-27** (1999) 310.
24. S-M. Moon and S-I. Pyun, *Corrosion* **54** (1998) 546.
25. C.M.A. Brett, *J. Appl. Electrochem.* **20** (1990) 1000.
26. H.A. El Shayeb, F.M. Abd El Wahab and S. Zein El Abedin, *Br. Corros. J.* **34** (1999) 37.
27. M. Pourbaix, 'Atlas of Electrochemical Equilibria in Aqueous Solutions', National Association of Corrosion Engineers, Houston, TX (1974).